Natural Convection in Gravity-Modulated Porous Layers

Saneshan Govender

Abstract We analyze natural convection in porous layers subjected to gravity modulation. In particular a linear stability analysis and weak non-linear analysis is presented for both synchronous and subharmonic solutions and the exact point for the transition from synchronous to subharmonic solutions is computed. It is demonstrated that increasing the excitation frequency rapidly stabilizes the convection up to the transition point from synchronous to subharmonic convection. Beyond the transition point, the effect of increasing the frequency is to slowly destabilize the convection.The weak-non-linear results show that increasing the excitation frequency rapidly decays the convection amplitude. An analogy between the inverted pendulum with an oscillating pivot point and the gravity modulated porous layer is developed and it is shown that the convection cell wavelength is related to the length of the pendulum.

1 Introduction

The classical Rayleigh–Benard problem has been extensively studied for both pure fluids and porous domains, with and without rotation. In both pure fluids and porous media, the density gradient becomes unstable and fluid motion results when a critical temperature difference, measured by means of the Rayleigh number, is exceeded. Comprehensive reviews are provided by Chandrasekar (1961) for pure fluids whilst Bejan (1995) provides a review of the fundamentals of heat convection in porous media.

The classical stability analysis no longer applies if the Rayleigh number (or the temperature difference) is time dependant. Time dependant body forces may occur in systems, with density gradients, subjected to vibrations. The influence of vibrations on thermal convection depends on the orientation of the time dependant acceleration with respect to the thermal stratification. Much work has been done for pure fluids for a vertically modulated fluid layer with constant vertical

S. Govender
University of Kwa-Zulu Natal, Durban, South Africa
e-mail: govenders65@ukzn.ac.za

P. Vadász (ed.), *Emerging Topics in Heat and Mass Transfer in Porous Media*,

stratification, i.e. modulated Rayleigh–Benard convection. Comprehensive analyses by Gresho & Sani (1970), Wadih & Roux (1988), Christov & Homsy (2001) and Hirata et al. (2001) are available for flow and heat transfer in a pure fluid layer subjected to gravity modulation. Alex & Patil (2002a, b), Bardan and Mojtabi (2000) and Bardan et al. (2004) provide the good references of work dealing with the effects of vibration on flow and heat transfer in porous media. In the latter two studies however, an averaging technique is used whereby the vibration body force is split into a steady and time dependant portion. It is also mentioned that with this method of solution, the subharmonic modes are never captured. Govender (2004, 2005a) utilises a direct method of solution and the resulting governing equation is cast into the canonical form of the much publicized Mathieu equation. The author then analyses the problem and recovers both the synchronous and subharmonic solutions in the parameter domain. In addition Govender (2005b) provides a comprehensive weak-nonlinear analysis for high frequency vibration. Also, Govender (2005c) provides an analysis for stability analyses for gravity modulation with heating from below whilst Govender (2005d) provides a stability analysis of low frequency vibration.

2 Problem Formulation

A shallow horizontal fluid saturated porous layer subject to vibration is presented in Fig. 1. The porous medium is constrained by rigid horizontal plates, spaced a distance H_* apart, and oscillates parallel to the gravitational field in the vertical direction. In addition the Darcy law is extended to include the time derivative while the Boussinesq approximation is applied to account for the effects of the density variations.

Subject to these conditions, the following dimensional set of governing equations for continuity, Darcy and energy, is proposed:

$$\nabla_* \cdot \boldsymbol{V}_* = 0, \tag{1}$$

$$\boldsymbol{V}_* = \frac{\boldsymbol{k}_*}{\mu_*}\left[-\nabla_* p_* - (\rho_* - \rho_{c^*})\left(g_* + b_*\omega_* \sin(\omega_* t_*)\right)\hat{e}_z - \frac{\rho_{c^*}}{\phi}\frac{\partial \boldsymbol{V}_*}{\partial t_*}\right], \tag{2}$$

$$\frac{\partial T_*}{\partial t_*} + \boldsymbol{V}_* \cdot \nabla_* T_* = \lambda_* \nabla_*^2 T_*. \tag{3}$$

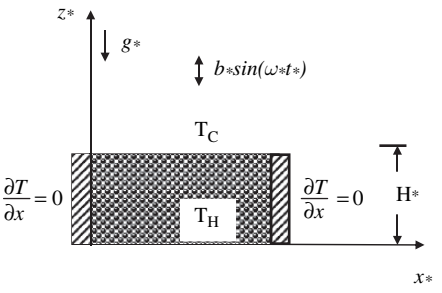

Fig. 1 Differentially heated porous layer subjected to vibration

It should be borne in mind that if the temperature effects are removed from Eq. (2), we obtain in the frequency domain a frequency dependant and complex valued permeability whose real and imaginary parts show a behaviour that resembles the Biot seepage law. The values λ_* / H_* , $\mu_* \lambda_* / k_{c^*}$ and $\Delta T_c = (T_H - T_C)$ are used to scale the filtration velocity components (u_*, v_*, w_*), reduced pressure (p_*), and temperature variations ($T_* - T_C$), respectively, where λ_* is the effective thermal diffusivity including the effect of the ratio between the heat capacity of the fluid and the effective heat capacity of the porous domain, μ_* is the fluid's viscosity and k_{c^*} is a characteristic permeability associated with the porous matrix. The height of the layer H_* is used for scaling the variables x_*, y_*, and z_*. Accordingly, $x = x_* / H_*$, $y = y_* / H_*$, and $z = z_* / H_*$. The time variable is scaled using H_*^2 / λ_* , hence $t = t_* \lambda_* / H_*^2$. In the current study a linear approximation was assumed for the relationship between the density and temperature, in the form $\rho_* = \rho_{c*} (1 - \beta_* \Delta T_c T)$ where β_* is the thermal expansion coefficient. Subject to the dimensional analysis, the following system of dimensionless equations result:

$$\nabla \cdot \boldsymbol{V} = 0, \tag{4}$$

$$\left(\frac{1}{Va} \frac{\partial}{\partial t} + 1 \right) \boldsymbol{V} = -\nabla p - R \left[1 + \delta \sin(\Omega t) \right] T \hat{e}_z, \tag{5}$$

$$\frac{\partial T}{\partial t} + \boldsymbol{V} \cdot \nabla T = \nabla^2 T. \tag{6}$$

The symbols $\boldsymbol{V}$, T and p represent the dimensionless filtration velocity vector, temperature and reduced pressure, respectively, and $\hat{e}_z$ is a unit vector in the z-direction. In Eq. (5), Ω is the scaled frequency, defined as $\Omega = \omega_* H_*^2 / \lambda_*$, whilst the non-dimensional amplitude δ is defined as $\delta = \kappa Fr \Omega^2$, where $\kappa = b_* / H_*$ and Fr is the modified Froude number defined as $Fr = \lambda_*^2 / (g_* H_*^3)$. The parameter Va is the Vadasz number, as pointed out by Straughan (2000), and includes the Prandtl and Darcy numbers as well as the porosity of the porous domain and is defined as

$$Va = \frac{\phi \, \mathrm{Pr}}{Da}. \tag{7}$$

In Eq. (7) $Pr = \nu_* / \lambda_*$ is the Prandtl number, $Da = k_{c^*} / H_*^2$ is the Darcy number, ϕ is the porosity and ν_* stands for the kinematic viscosity of the fluid. It is only through this combined dimensionless group that the Prandtl number affects the flow in the porous media, see Vadasz (1998) for a full discussion on the numerical values that Pr can assume in a typical porous medium. In Eq. (5) one also observes the Rayleigh number, R; defined as $R = \beta_* \Delta T_C g_* k_{c^*} H_* / \nu_* \lambda_*$. As all boundaries are rigid, the solution must follow the impermeability conditions there, i.e. $\boldsymbol{V} \cdot \hat{e}_n = 0$ on the boundaries, where $\hat{e}_n$ is a unit vector normal to the boundary. The temperature boundary conditions are: $T = 1$ *at* $z = 0$, $T = 0$ *at* $z = 1$ and $\nabla T \cdot \hat{e}_n = 0$ on all other walls representing the insulation condition on these walls. The partial differential equations (4–6) forms a non-linear coupled system which together with the corresponding boundary conditions accepts a basic motionless solution with a

parabolic pressure distribution. The solutions for the basic temperature and flow field is given as, $T_B = 1 - z$ and $\boldsymbol{V_B} = 0$. To provide a non-trivial solution to the system it is convenient to apply the curl operator $(\nabla\times)$ twice on Eq. (5) and consider the z-component, to obtain,

$$\left(\frac{1}{Va}\frac{\partial}{\partial t} + 1\right)\nabla^2 \boldsymbol{V} + R\left[1 + \delta\sin(\Omega t)\right]\nabla_H^2 T\hat{e}_z = 0, \tag{8}$$

for a solenoidal velocity field, Eq. (4). The Laplacian operator in Eq. (8) is defined as $\nabla_H^2 \equiv \partial^2/\partial x^2 + \partial^2/\partial y^2$ for cartesian co-ordinates.

3 Linear Stability Analysis

The basic motionless solution is $\boldsymbol{V_B} = 0$ and $T_B = 1 - z$. Assuming small perturbations around the basic solution in the form $\boldsymbol{V} = \boldsymbol{V}_B + \boldsymbol{V}'$ and $T = T_B + T'$, and linearising equations (6) and (8) yields the following linear system,

$$\left(\frac{1}{Va}\frac{\partial}{\partial t} + 1\right)\nabla^2 \boldsymbol{V}' + R\left[1 + \delta\sin(\Omega t)\right]\left[\frac{\partial^2 T'}{\partial x\partial z}\hat{e}_x + \frac{\partial^2 T'}{\partial y\partial z}\hat{e}_y - \nabla_H^2 T'\hat{e}_z\right] = 0, \tag{9}$$

$$\left[\frac{\partial}{\partial t} - \nabla^2\right]T' - w' = 0, \tag{10}$$

where w' is the perturbation to the vertical component of the filtration velocity. The boundary conditions in the $z-$direction required for solving Eqs. (9) and (10) are $w' = T' = 0$ at $z = 0$ and $z = 1$. In the x-direction $\partial T/\partial x = 0$ at $x = 0$ and $x = L$. The coupling between Eqs. (9) and (10) can be removed by considering the vertical component of Eq. (9) and eliminating w' to provide one equation for the temperature perturbation in the form

$$\left(\frac{1}{Va}\frac{\partial}{\partial t} + 1\right)\nabla^2\left[\frac{\partial}{\partial t} - \nabla^2\right]T' - R\left[1 + \delta\sin(\Omega t)\right]\nabla_H^2 T' = 0. \tag{11}$$

Assuming an expansion into normal modes in the x- and y-directions, and a time-dependant amplitude $\theta(t)$ of the form,

$$T' = \theta(t)\exp\left[i\left(s_x y + s_y z\right)\right]\sin(\pi z) + c.c, \tag{12}$$

where $c.c.$ stands for the complex conjugate terms and $s^2 = s_x^2 + s_y^2$. Substituting Eq. (12) into the Eq. (11) provides an ordinary differential equation for the amplitude $\theta(t)$,

$$\frac{d^2\theta}{dt^2} + 2p\frac{d\theta}{dt} - F(\alpha)\gamma\left[\left(\tilde{R} - \tilde{R}_o\right) + \tilde{R}\delta\sin(\Omega t)\right]\theta = 0, \tag{13}$$

where $\alpha = s^2/\pi^2$, $\gamma = Va/\pi^2$ and $\tilde{R} = R/\pi^2$. In Eq. (13), $2p = \pi^2(\alpha + 1 + Va)$, $F(\alpha) = \pi^4\alpha/(\alpha + 1)$ and $\tilde{R}_o$ is the un-modulated Rayleigh number defined as $\tilde{R}_o = (\alpha + 1)^2/\alpha$. Using the transformation $t = (\pi/2 + 2\tau)/\Omega$, equation (13) may be cast into the canonical form of the Mathieu equation, as outlined by McLachlan (1964), and is given as

$$\frac{d^2X}{d\tau^2} + [a + 2q\cos(2\tau)]\,X = 0. \tag{14}$$

The solution to Eq. (14) follows the form $X = G(\tau)\,e^{\sigma\tau}$ where $G(\tau)$ is a periodic function with a period of π or 2π and σ is a characteristic exponent which is a complex number and is a function of a and q respectively. In this chapter the definitions for a, q and σ are obtained upon transforming Eq. (13) to the canonical form and is defined as,

$$\frac{2}{\sqrt{-a}} = \frac{\Omega}{\left[F(\alpha)\,\gamma\left(\tilde{R} - \eta\right)\right]^{1/2}}, \tag{15}$$

$$\frac{1}{2}q = \frac{F(\alpha)\,\gamma\tilde{R}\delta}{\Omega^2} = F(\alpha)\,\gamma\tilde{R}\kappa Fr, \tag{16}$$

$$\sigma = -2p/\Omega, \tag{17}$$

where η is a parameter defined as,

$$\eta = -\tilde{R}_o\frac{(\alpha + 1 - \gamma)^2}{4\gamma(\alpha + 1)}. \tag{18}$$

When $\sigma = \sigma_r = 0$, the solution to Eq. (14) is defined in terms of Mathieu functions, c_n and d_m, such that for each Mathieu function, c_n and d_m, there exists a relation between a and q. This relationship is shown in Fig. 2 for the Mathieu functions d_0, c_1 and d_1 for small values of q.

It is observed from Fig. 2 that d_0, c_1 and d_1 separates the stable and unstable solutions. If the other Mathieu functions (viz. c_n and d_m where $n = 2, 3, 4..N$ and $m = 2, 3, 4, ..M$) are superimposed on Fig. 2 one would observe that the regions separated by the Mathieu functions in the a–q plane are alternately stable and unstable. For our analysis we consider only small values of q, so the analysis around the Mathieu functions d_0, c_1 and d_1 is sufficient. Upon examining Fig. 2, one is able to note that the region below curve d_0, and the region enclosed between curves c_1 and d_1 correspond to the unstable zones. The narrow region between curves d_0 and c_1 represent the stable zones. In principle the regions enclosed by even indices of d_m (i.e. $m = 0, 2, 4, 6..$) yields synchronous solutions whilst those regions enclosed by odd indices of d_m (i.e. $m = 1, 3, 5, 7..$) yields subharmonic solutions thus implying that the a–q plane consists of alternating regions of synchronous and subharmonic solutions. In the stable regions of Mathieu's equation, σ is complex with a negative real part. Since σ is a function of a and q, which are dependant on γ, $\tilde{R}$, α, δ and Ω,

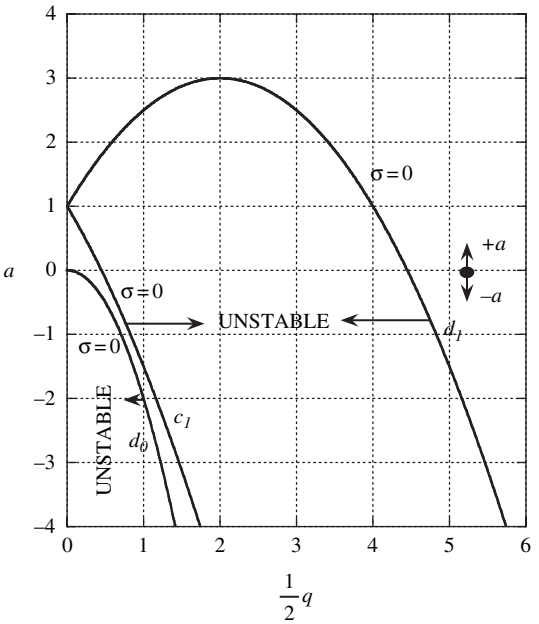

Fig. 2 Mathieu chart clearly demarcating the stable and unstable zones

the stability porous layer is also seen to depend on these variables as well. In addition there are solutions to Eq. (14) for $a > 0$ and $a < 0$; also, q may be replaced by $-q$ with no effect on the solution. In this study for a porous medium heated from below the numerical values for a are less than zero and are defined by Eq. (15). In the case of liquid metals, as found during the solidification of binary alloys, see Pillay & Govender (2005), we may propose for a Lead-Antimony (Pb-Sn) system, $\lambda_* = 1.08 \times 10^{-5}\,\mathrm{m^2/s}$, $\nu_* = 2.47 \times 10^{-7}\,\mathrm{m^2/s}$, and $Pr = 2.3 \times 10^{-2}$. For a characteristic height $H_* = 0.1\,m$, we find that the corresponding value for the Froude number, Fr, is $Fr = 1.1 \times 10^{-3}$. If the vibration amplitude to characteristic height ratio κ is $\kappa = 10^{-2}$, then the parameter $(\kappa Fr) = O\left(10^{-5}\right)$. As a result we note that q assumes very small values for the above property values. For the low Prandtl number liquid melt, we follow Vadasz (1998) and propose that $Va = O(1)$, thereby allowing for the retention of the time derivative in the Darcy equation. In the current study we propose the following definition for the modified characteristic exponent: $\xi = \sigma/\sqrt{-a}$. A chart of $1/2q$ versus $2/\sqrt{-a}$, for various values of ξ, is shown in Fig. 3 for small values of q, see McLachlan (1964). In Fig. 3, $\xi = 0$ refers to the Mathieu function solution depicted by the curves for d_0, c_1 and d_1 in Fig. 3. We may now present a relation for the characteristic Rayleigh number in terms of the newly defined parameter ξ, by substituting $\xi = \sigma/\sqrt{-a}$ in Eq. (15), and rearranging yields,

$$\tilde{R} = \eta + \frac{\left(\tilde{R}_o - \eta\right)}{\xi^2}. \tag{19}$$

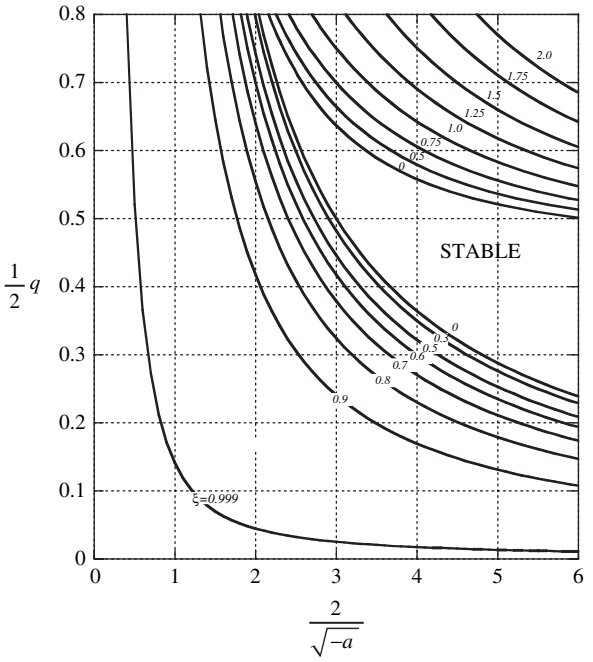

Fig. 3 Mathieu chart for the synchronous and sub-harmonic zones

Figure 3 together with Eqs. (15)–(19) may be used to evaluate the critical Rayleigh number and wavenumber ($\alpha_{cr} = \left(\alpha_x + \alpha_y\right)_{cr}$) in terms of the frequency Ω, the parameters (κFr) and γ.

We proceed by first evaluating the characteristic Rayleigh number versus the frequency for $\gamma \approx O(3)$ and $(\kappa Fr) = O\left(10^{-5}\right)$ and selected values of the wavenumber according to the following method: (a) select a value of ξ, (b) evaluate $\tilde{R}$ using Eq. (19), (c) compute the value for $1/2q$ using Eq. (16), (d) read $2/(-a)^{1/2}$ from Fig. 2, and (e) evaluate the frequency from Eq. (15). A series of curves of the critical Rayleigh number versus the frequency may be plotted for various wavenumbers and an example of such a curve is shown in Fig. 4 for $\alpha = 0.3$. Using Fig. 4 we evaluate the critical wavenumber and Rayleigh number corresponding to each wavenumber across the frequency range. The critical Rayleigh number and wavenumber as a function of the frequency is shown in Fig. 5, and shows that gravity modulation stabilizes the convection for the region of synchronous response but slowly destabilizes convection for the region of subharmonic response.

The stabilizing effect of vibration is small at low frequencies, but becomes significant for larger frequencies. Figure 5 also shows that close to $\Omega_t \cong 1225$, the Rayleigh number curve changes from a rapidly increasing trend to a slowly decreasing trend. The critical wavenumber is also seen to decrease with increasing frequencies, for both the regions of synchronous and subharmonic response. It is notable that upon transition from synchronous to subharmonic solutions there is a rapid increase in the critical wavenumber.

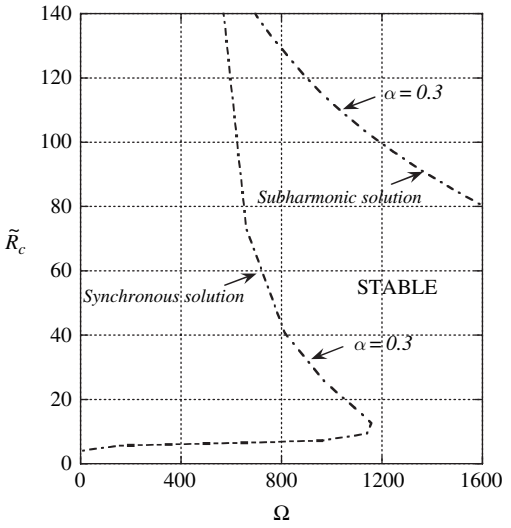

Fig. 4 Characteristic Rayleigh and wave number versus frequency

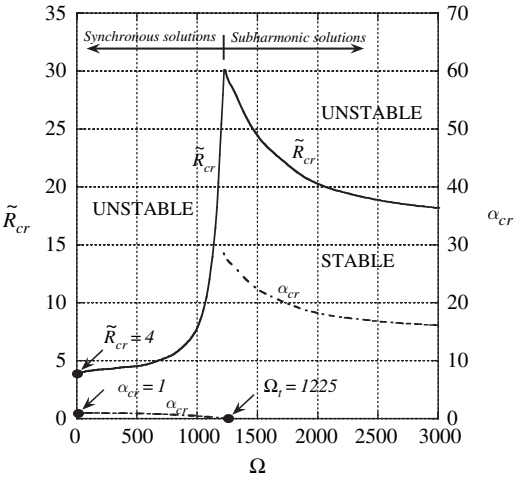

Fig. 5 Critical Rayleigh and wave number versus frequency

4 Weak Non-linear Anlaysis

Govender (2005b) provides a weak non-linear analysis in order to determine quantitatively the amplitude of convection. It is convenient to use the definition of the stream function in the form $u = \partial\psi/\partial z$; $w = -\partial\psi/\partial x$, and Govender (2005b) presents Eqs. (1–3) in terms of the stream function and temperature as follows for slow time scale variations,

$$\left(\frac{1}{Va}\frac{\partial}{\partial t} + 1\right)\nabla^2\psi + Ra\,(1 + \delta\sin(\Omega t))\,\frac{\partial T}{\partial x} = 0, \tag{20}$$

$$\frac{\partial T}{\partial t} + \frac{\partial \psi}{\partial z}\frac{\partial T}{\partial x} - \frac{\partial \psi}{\partial x}\frac{\partial T}{\partial z} = \nabla^2 T, \tag{21}$$

where the definition of the Laplacian operator is given as $\nabla^2 = \partial^2/\partial x^2 + \partial^2/\partial z^2$. The stream function, temperature and amplitude δ may be expanded in terms of a small parameter ε, defined as $\varepsilon = \left[Ra/Ra_{cr} - 1\right]^{1/2}$, as follows:

$$[\psi, T] = [\psi_B, T_B] + \varepsilon\,[\psi_1, T_1] + \varepsilon^2\,[\psi_2, T_2] + \varepsilon^3\,[\psi_3, T_3] + O(\varepsilon^4), \tag{22}$$

$$\delta = \delta_0 + \varepsilon\delta_1 + \varepsilon^2\delta_2 + . \tag{23}$$

The expansion (23) is consistent with the basic solution ($T_B = 1 - z$ and $\boldsymbol{V_B} = 0$) provided that δ_0 vanishes at the lowest order. In addition, unless δ_1 vanishes, the equations obtained at order ε and ε^2 present a singularity in the solution. These observations indicate that the effects of vibration should be introduced at the lowest possible order i.e., $\delta \approx \varepsilon^2\delta_1$, thereby enabling consistency. By using the definition for ε given above, the Rayleigh number may be expanded as $Ra = Ra_{cr}(1 + \varepsilon^2)$, where $Ra_{cr} = 4\pi^2$ is the critical Rayleigh number for a porous layer heated from below and subjected to gravity only. In addition we allow time variations only at the slow time scale $\tau = \varepsilon^2 t$ in order to prevent exponential growth and reaching finite values for the amplitude at the steady state. Substituting the expansion (22), as well as the slow time scale, just defined, into the system (20), (21) and equating like powers of ε produces a hierarchy of linear partial differential equations to each order.

$$\left(\frac{\varepsilon^2}{Va}\frac{\partial}{\partial \tau} + 1\right)\nabla^2\psi_m + Ra_{cr}\,(1 + \delta\sin(\Omega_0\tau))\,\frac{\partial T_m}{\partial x} = H_m, \tag{24}$$

$$\varepsilon^2\frac{\partial T_m}{\partial \tau} + \frac{\partial \psi_m}{\partial z}\frac{\partial T_m}{\partial x} - \frac{\partial \psi_m}{\partial x}\frac{\partial T_m}{\partial z} - \nabla^2 T_m = J_m, \tag{25}$$

where $\Omega_0 = \Omega/\varepsilon^2$ represents the large frequency scaling. To order, ε, $H_1 = J_1 = 0$ and the solution at order ε is given by

$$\psi_1 = A_1\sin(sx)\sin(\pi z),\ T_1 = B_1\cos(sx)\sin(\pi z). \tag{26}$$

The relationship between the amplitudes is obtained by substituting Eq. (26) in the system (24), (25) and is found to be

$$A_1 = -\pi\frac{(\alpha + 1)}{\sqrt{\alpha}}B_1. \tag{27}$$

The amplitude A_1 remains undetermined at this stage, and will be determined from a solvability condition of the order $O(\varepsilon^3)$ equations at order ε^3. The critical Rayleigh number and wavenumber to the leading order are found to be $R_{cr} = 4$ and $\alpha_{cr} = 1$. The equations to order ε^3 yields a solvability condition which constrains the amplitude

of the solution at order ε and enables its determination. The solvability condition is obtained by decoupling the governing equation at order ε^3 to yield a single non-homogenous partial differential equation for T_3 with corresponding forcing functions which include the $O(\varepsilon)$, and $O\left(\varepsilon^2\right)$ solutions (Govender 2005b) as follows,

$$\nabla^4 T_3 + Ra_{cr}\frac{\partial^2 T_3}{\partial x^2} = \frac{\partial H_3}{\partial x} + \nabla^2 J_3, \tag{28}$$

$$\text{where } H_3 = -\left(Ra_{cr}(t)\frac{\partial T_1}{\partial x} + \frac{1}{Va}\frac{\partial \nabla^2 \psi_1}{\partial \tau}\right), \tag{29}$$

$$\text{and, } J_3 = \frac{\partial T_1}{\partial \tau} + \frac{\partial \psi_1}{\partial z}\frac{\partial T_2}{\partial x} + \frac{\partial \psi_2}{\partial z}\frac{\partial T_1}{\partial x} - \frac{\partial \psi_1}{\partial x}\frac{\partial T_2}{\partial z} - \frac{\partial \psi_2}{\partial x}\frac{\partial T_1}{\partial z}. \tag{30}$$

Setting the coefficients of the secular terms in Eq. (28) to zero, yields the following Ginzburg–Landau equation for the leading order $O(\varepsilon)$ amplitude,

$$\frac{dB}{dt} = \mu_0\left(1 + \delta_1 \sin(\Omega t)\right)B - \chi B^3, \tag{31}$$

where $B = \varepsilon B_1$. The following notation is used in Eq. (31),

$$\mu_0 = \chi\xi, \quad \chi = \frac{\pi^4\gamma(\alpha+1)^2}{4(\alpha+1+\gamma)}, \xi = \frac{4R_{cr}\alpha}{\pi^2(\alpha+1)^3}\varepsilon^2. \tag{32}$$

Equation (31) is in the form of Bernoulli's differential equation and the solution to this type of equation is of the form,

$$B = \frac{e^{\mu_0\left(t-\delta_1/\Omega\cos(\Omega t)\right)}}{\left[2\chi\int e^{\mu_0\left(t-\delta_1/\Omega\cos(\Omega t)\right)}dt + C_1\right]}, \tag{33}$$

where $B(0) = b_0$ and C_1 is an integration constant. When $\delta_2 \to 0$, the analytical solution to Eq. (33) is given as ,

$$B = \frac{b_0\xi^{1/2}e^{\mu_0 t}}{\left[\xi - b_0^2\left(1 - e^{2\mu_0 t}\right)\right]^{1/2}}. \tag{34}$$

When $t \to \infty$, the classic steady state solution is found to be $B = 0$ or $B = b_0\left/|b_0|\xi^{1/2}\right.$. If $\delta_2 \neq 0$, we observe that the integral in Eq. (34) cannot be evaluated to obtain a closed form solution, and it is for this reason that we resort to a numerical solution of Eq. (34) by adopting the Runge–Kutte method. For a time step of 0.079 it was shown by Govender (2005b) that the analytical and numerical solutions were in perfect agreement for the case of no vibration ($\delta_2 = 0$). A time step of 0.079, will be retained for simulations corresponding to $\delta_2 \neq 0$. Figure 6 shows the amplitude B versus time for $\Omega = 0$, $\Omega = 100$ and $\Omega = 250$.

It can be clearly seen that increasing the frequency from $\Omega = 0$ to $\Omega = 100$ reduces the convection amplitude B. For $\Omega = 250$, it can be observed that for $t > \approx 7.5$, the conduction solution ($B = 0$) is stable. Figure 7 shows the amplitude B versus time for $\Omega = 0$, $\Omega = 300$ and $\Omega = 350$.

It can be seen for $\Omega = 300$ that beyond $t \approx 20$ the conduction solution is stable, whilst for $\Omega = 350$, the conduction solution sets in as the stable mode as early as $t \approx 2.5$. Figure 8 shows the amplitude B versus time for $\Omega = 0$, $\Omega = 370$ and $\Omega = 450$. Figure 8 shows that the conduction solution is stable beyond $t \approx 5$ for $\Omega = 370$ and $\Omega = 450$. Further simulations were performed for $\Omega = 500$, $\Omega = 750$, $\Omega = 1500$ and $\Omega = 3000$, and it was discovered that the basic solution

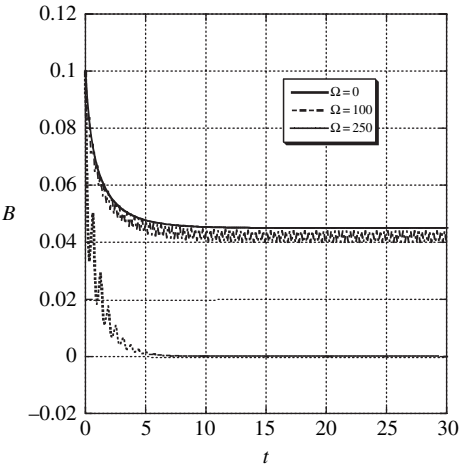

Fig. 6 Convection amplitude B versus time t for $\Omega = 0, 100, 250$

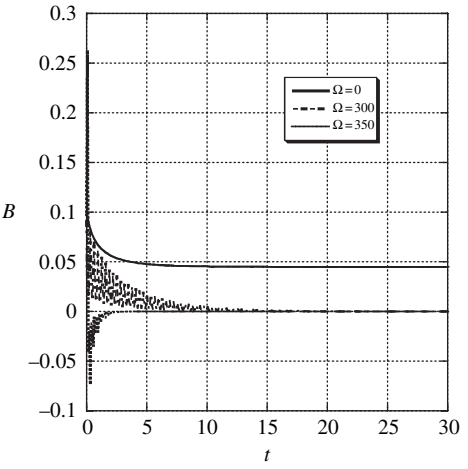

Fig. 7 Convection amplitude B versus time t for $\Omega = 0, 300, 350$

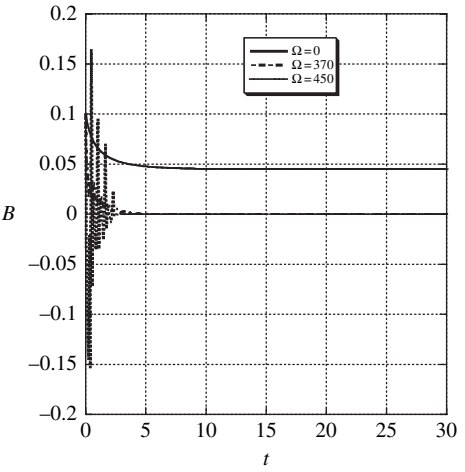

Fig. 8 Convection amplitude B versus time t for $\Omega = 0, 370, 450$

($B = 0$) is the only possible solution. The results depicted in Figs. 6–8 clearly indicate that increasing the vibration frequency stabilizes the convection by causing the convection amplitude to approach zero.

5 Pendulum Analogy

Govender (2006) demonstrated that the temperature in a porous layer heated from below may be likened to the motion of an inverted pendulum with an oscillating pivot point. Figure 9 below shows the inverted pendulum that will be considered. With reference to Fig. 9, one may write the net velocity as,

$$\vartheta^2 = (L\dot{\varphi})^2 + \dot{y}^2 - 2L\dot{\varphi}\dot{y}\sin\varphi. \tag{35}$$

Using the above definition we may write the equations for the kinetic, damping and potential energies respectively:

$$\text{Kinetic energy} : KE = \frac{1}{2}m\left((L\dot{\varphi})^2 + \dot{y}^2 - 2L\dot{\varphi}\dot{y}\sin\varphi\right), \tag{36}$$

$$\text{Damping energy} : DE = \frac{1}{2}c\left((L\dot{\varphi})^2 + \dot{y}^2 - 2L\dot{\varphi}\dot{y}\sin\varphi\right), \tag{37}$$

$$\text{Potential energy} : PE = -\left(mgL\left(1 - \cos\varphi\right) + mgy\right). \tag{38}$$

Substituting in Lagranges equation,

$$\frac{d}{dt}\left(\frac{\partial KE}{\partial\dot{\varphi}}\right) - \frac{\partial KE}{\partial\varphi} + \frac{\partial PE}{\partial\varphi} + \frac{\partial DE}{\partial\varphi} = 0, \tag{39}$$

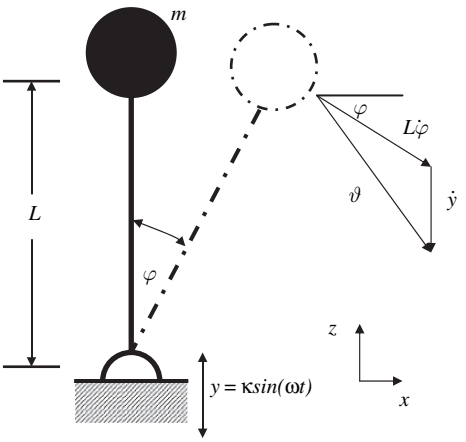

Fig. 9 The inverted pendulum with an oscillating pivot point

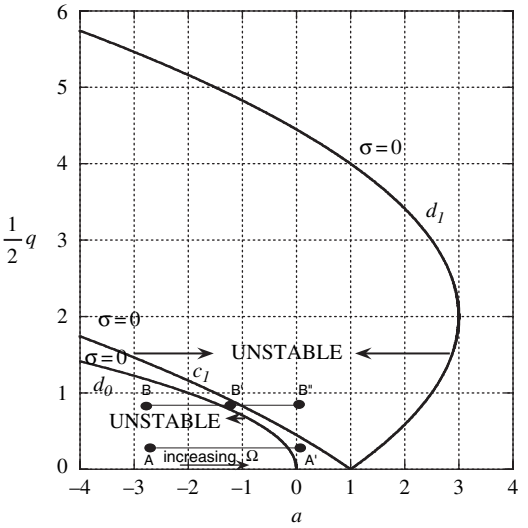

Fig. 10 Mathieu chart showing the stability of an inverted pendulum

and simplifying the result yields,

$$\frac{d^2\varphi}{dt^2} + 2\lambda\Omega_n \frac{d\varphi}{dt} - \left[\Omega_n^2 + 2\lambda\Omega_n\Omega\frac{\kappa}{L}\cos(\Omega t) - \Omega^2\frac{\kappa}{L}\sin(\Omega t)\right]\varphi = 0, \qquad (40)$$

which represents the equation for the motion of the inverted pendulum of length L with an oscillating pivot point, where the vertical motion of the pivot is given as $\kappa \sin(\Omega t)$. The above equation for the pendulum motion is valid for planar motion at small angles φ from the vertical. Also the un-damped natural frequency is given as $\Omega_n = \sqrt{g_*/L}$,

and the damping ratio is defined as $\xi_0 = c/2m\Omega_n$. Both Eqs. (13) and (40) may be cast into the canonical form of the Mathieu equation, as outlined by McLachlan (1964), and is given as

$$\frac{d^2X}{d\tau^2} + [a + 2q\cos(2\tau)]\,X = 0. \tag{41}$$

The solution to Eq. (41) follows the form $X = \theta(\tau)\,e^{\sigma\tau}$ where $\theta(\tau)$ is a periodic function with a period of π or 2π and σ is a characteristic exponent which is a complex number and is a function of a and q respectively. Incidentally the damping terms in Eqs. (13) and (40) has a stabilizing effect on the solutions and the exponential behavior is no longer of the form $e^{\sigma t}$. Following McLachlan (1964): for the pendulum, the argument of the exponential factor is $\left(1/2\cdot\sigma\cdot\Omega/\Omega_n - \xi_0\right)\Omega_0 t$, whilst for the gravity modulated porous layer heated from below, the argument of the exponential factor is $\left(1/2\cdot\sigma\Omega - p\right)t$. The stability criterion for the inverted pendulum is of the form $\xi_0 \geq 1/2\cdot\sigma\cdot\Omega/\Omega_n$ whilst for the gravity modulated porous layer $p \geq 1/2\cdot\sigma\Omega$. For the inverted pendulum with an oscillating pivot point:

$$\frac{2}{\sqrt{-a}} = \frac{1}{\left(\frac{\Omega_n}{\Omega}\right)\left(1+\xi_0^2\right)^{1/2}},\ \frac{1}{2}q = \frac{\delta}{L},\quad \sigma = 2\Omega_n/\Omega. \tag{42}$$

Equating the relations for $1/2q$ for both the oscillating porous layer and the pendulum, and noting that $\Delta T_C = \Delta\rho/\rho << 1$ yields, $1/2\ q = \kappa/L = F(\alpha)\,\gamma\tilde{R}\kappa Fr = F(\alpha)\cdot\kappa\cdot\phi_*/\pi^4\cdot\beta_*\Delta T_C$, which implies that the roll cell behaves like a very long pendulum with an effective dimensionless length of $L = 1/\left(F(\alpha)\cdot\kappa\cdot\phi_*/\pi^4\cdot\beta_*\Delta T_C\right)$. Rewriting Eq. (11) as, $a = -4\left(\Omega_n/\Omega\right)\left(1+\xi_0^2\right)^{1/2}$, one clearly observes that as Ω is increased, the absolute value for a gets smaller and smaller, up to a point when a is identically zero, at which point the frequency $\Omega \to \infty$. Choosing some exploratory value for δ/L (or $1/2q$) in Fig. 10, we may observe, by means of reference plane $A - A'$ which straddles the unstable and stable zones, the effects of frequency of oscillation Ω. Point A is incidentally in the unstable zone whilst point A' is in the stable zone. Increasing the frequency from some small/moderate value at point A in the unstable zone allows a shift towards point A' in the stable zone. This clearly shows that a, statically unstable, inverted pendulum may be stabilized by oscillating the pivot point in the vertical plane at some frequency Ω. However if some larger value of δ/L (or $1/2q$) is selected, say $\delta/L = 1$, we observe by means of reference plane $B - B' - B''$,which straddles the unstable; stable; and unstable zones respectively, that although increasing the frequency stabilizes the inverted pendulum up to point B', very large pivot frequencies tends to destabilize the inverted pendulum. In essence we have observed via the second case that for larger values of $1/2q$ a transition from synchronous to subharmonic solutions may occur as observed by Govender (2005a, b) for the gravity modulated porous layer heated from below.

The following analogy is thus evident: The temperature in a gravity modulated porous layer heated from below ($R > 0$, "top heavy"-unstable) is similar to the motion of a simple pendulum with an oscillating pivot point (inverted – unstable).

6 Conclusion

The author presents results dealing with the investigation of the effect of gravity modulation on the stability of convection in a differentially heated porous layer with particular focus on the transition from synchronous to subharmonic solutions. In addition a weak non linear analysis is also presented together with the development of an analogy between the oscillating porous layer and a pendulum. The linear stability analysis is performed with the aid of the Mathieu stability charts and it is discovered that gravity modulation stabilizes the convection for the region of synchronous solutions but slowly destabilizes convection for the region of subharmonic solutions. The transition point from synchronous to subharmonic solutions is found to be $\Omega_t \cong 1225$. It is proposed that the results of the current work may be extended for use in the investigation of the stability of solutal convection in solidifying mushy layers, with a view to preventing the onset of freckle formation in binary alloys, Pillay & Govender (2005)

Analytical results are also presented for the weak non-linear analysis which included an extended Darcy equation formulation. The numerical results revealed that increasing the frequency of vibration causes the amplitude of convection to approach zero, i.e. vibration stabilizes the convection.

Finally the author also showed that an analogy exits between the gravity modulated porous layer heated from below and the inverted pendulum with an oscillating pivot point. It is shown that the temperature in a gravity modulated porous layer subjected to vibration ($R > 0$-"top heavy" unstable) may be likened to the motion of a pendulum (inverted-unstable). In addition it was also pointed out that the roll cell behaves similar to a very long pendulum.

Acknowledgments The author would like to dedicate this exposition to his daughter Miss Sumithra Govender, who was born on 11 August 2006.

References

Alex, S.M. & Patil, R.: (2002a), Effect of variable gravity field on thermal instability in a porous medium with inclined temperature gradient and vertical throughflow, *J. Porous Media* **5**, 137–147.

Alex, S.M. and Patil, R.: (2002b), Effect of variable gravity field on convection in an anisotropic porous medium with internal heat source and inclined temperature gradient, *ASME J. Heat Transfer* **124**, 144–150.

Bardan, G and Mojtabi, A. (2000) On the Horton–Rogers–Lapwood convective instability with vertical vibration: onset of convection, *Phys. Fluids* **12**, 2723–2731.

Bardan, G, Razi, Y.P. & Mojtabi, A. (2004) Comments on the mean flow averaged model, *Phys. Fluids* **16**, 4535–4538.

Bejan, A.: (1995), *Convection Heat Transfer*, 2nd ed., Wiley, New York.
Chandrasekar, S.: (1961), *Hydrodynamic and Hydromagnetic Stability*, Oxford University Press, Oxford.
Christov, C.I. & Homsy, G.M.: (2001), Nonlinear dynamics of two-dimensional convection in a vertically stratified slot with and without gravity modulation, *J. Fluid Mech* **430**, 335–360.
Govender, S.: (2004), Stability of convection in a gravity modulated porous layer heated from below, *Trans. Porous Media* **57** (2), 113–123.
Govender S.: (2005a), Linear stability and convection in a gravity modulated porous layer heated from below: Transition from synchronous to subharmonic solutions, *Trans. Porous Media* **59** (2), 227–238.
Govender S.: (2005b), Weak non-linear analysis of convection in a gravity modulated porous layer, *Trans. Porous Media* **60** (1), 33–42.
Govender S.: (2005c), Destabilising a fluid saturated gravity modulated porous layer heated from above, *Trans. Porous Media* **59** (2), 215–225.
Govender S.: (2005d), Stability analysis of a porous layer heated from below and subjected to low frequency vibration: Frozen time analysis, *Trans. Porous Media* **59** (2), 239–247.
Govender S.: (2006), An analogy between a gravity modulated porous layer heated from below and the inverted pendulum with an oscillating pivot point, *Trans. Porous Media*, In Press.
Gresho, P.M. & Sani, R.L.: (1970), The effects of gravity modulation on the stability of a heated fluid layer, *J. Fluid Mech.* **40**, 783–806.
Hirata, K., Sasaki, T. & Tanigawa, H.: (2001), Vibrational effect on convection in a square cavity at zero gravity, *J. Fluid Mech.* **455**, 327–344.
McLachlan, N.W.: (1964), *Theory and Application of Mathieu Functions*, Dover, New York.
Pillay S.K. & Govender S.: (2005), Stability of convection in a gravity modulated mushy layer during the solidification of binary alloys, *Trans. Porous Media* **60** (2), 183–197.
Straughan, B.: (2000), A sharp nonlinear stability threshold in rotating porous convection, *Proc. R. Soc. Lond. A* **457**, 87–93.
Vadasz, P.: 1998, Coriolis effect on gravity-driven convection in a rotating porous layer heated from below, *J. Fluid Mech* **376**, 351–375.
Wadih, M. & Roux, B.: (1988), Natural convection in a long vertical cylinder under gravity modulation, *J. Fluid Mech* **193**, 391–415.